Available online at www.sciencedirect.com

ScienceDirect

Ceramics International 35 (2009) 3421–3425

CERAMICS INTERNATIONAL

www.elsevier.com/locate/ceramint

Correlation between yttria stabilized zirconia particle size and morphological properties of NiO–YSZ films prepared by spray coating process

A.C. Nascimento, R.M.F. Basaglia, F.T.A. Cunha, C.G. Fonseca, M.C. Brant, T. Matencio, R.Z. Domingues *

Departamento de Química, Instituto de Ciências Exatas, Universidade Federal de Minas Gerais, Av. Antônio Carlos, 6627,
CEP: 31270-901 Belo Horizonte, MG Brazil

Received 1 October 2008; received in revised form 4 May 2009; accepted 12 June 2009
Available online 7 July 2009

Abstract

A systematic approach was taken to investigate the morphology of NiO–yttria stabilized zirconia (YSZ) films deposited by a spray coating process. The final morphological aspects of anode films were influenced by the particle size of YSZ powders and the milling time of the slurries used for film deposition. YSZ powders with average particle size of 17 and 52 nm were obtained from powders calcined at 800 and 1000 °C, respectively. The results obtained by rheological studies pointed out that slurries prepared from YSZ powders calcinated at 1000 °C and milling time of 20 h had more stability. All slurries presented thixotropic and pseudoplastic behaviors.

Keywords: Solid oxide fuel cell (SOFC); Anode; Microstructure; NiO/YSZ

1. Introduction

Solid oxide fuel cells (SOFCs), are electrochemical devices that can convert the chemical energy of a fuel into electrical energy without pollution [1–3]. Due to their higher operating temperatures (700–1000 °C) these devices can use several kinds of fuels such as hydrogen, natural gas, and ethanol [4], and also can be used with high efficiency in cogeneration systems [5,6]. However, the performance of SOFCs depends on both the electrodes and electrolyte materials and their processing, besides another factors. Single cells are constructed with layered electrodes and include functional and current collector layers on both cathodic and anodic ends [7–9]. The functional layer is responsible for electrochemical reactions and thus must provide the active sites where the triple contact between electronic and ionic conductors and the gaseous phase (the triple phase boundary) takes place [10,11]. Ni–yttria stabilized zirconia (Ni/YSZ) is the most widely used anode material for SOFC in which YSZ is used as the electrolyte [12,13]. The utilization of this composite instead of pure Ni improves the electrolyte/anode contact area by minimizing the differences of thermal dilatation coefficients of metallic and ceramic materials and by increasing the number of sites where the electrochemical reaction can occur [14]. The anode composite has the desired requirements for an SOFC anode: YSZ acts as a matrix to Ni grains and inhibits Ni coalescence and aggregation [15,16], and Ni has high electrical conductivity and is an excellent catalyst for hydrogen oxidation [17–19]. The electrochemical performance of an anode is described elsewhere as being very dependent on its microstructure [20,21], thickness, porosity [22] and composition [23].

For anode films deposited by a spray [17,24] or tape casting processes [2], a slurry is usually prepared in two steps. Initially, ceramic powders of a given particle size are pre-homogenized together with the dispersant in a suitable solvent in a ball milling for a certain time, and then further organic additives such as binders and plasticizers, are added in adequate quantities. The resulting slurry is milled again for an additional time [25,26].

The film performance is, besides other factors, determined by its homogeneity [27], adherence and porosity. These

---

* Corresponding author. Tel.: +55 31 3409 5770; fax: +55 31 3409 5700.
E-mail address: rosanazd@ufmg.br (R.Z. Domingues).

0272-8842/$36.00
doi:10.1016/j.ceramint.2009.06.003

parameters are influenced by the conditions of slurries preparation and also by the powders' characteristics. Particle sizes before and after milling, the powder amount used during the slurry preparation, specific surface area [28] and milling time [29] are the more important parameters. They are responsible for the rheological behavior which is an efficient tool to predict the sinterability and microstructure of films.

Mechanical and electrochemical performances of the deposited films are enhanced if higher homogeneous and stable suspensions are used [25]. The rheological parameters are valuable data to provide control parameters of slurry quality. The present work evaluates how the parameters such as time of milling and the calcination temperature of YSZ powders influence on the slurry rheological properties and microstructure of anode NiO/YSZ films deposited by a spray coating process.

2. Experimental

2.1. Starting materials

YSZ (8 mol% yttria) powders were prepared by a co-precipitation method [30,31] using zirconium (IV) butoxide (Fluka) and yttrium oxide (Sigma) as starting materials. After this first step, the powder was separated into two aliquots which were calcined at 800 and 1000 °C (YSZ800 and YSZ1000), in order to obtain YSZ powders with different particle sizes.

YSZ/NiO composites were prepared by an impregnation method [32,33] using the previously prepared YSZ800 and YSZ1000 powders and nickel (II) nitrate hexahydrate (Sigma–Aldrich). The two composites obtained were named as NiOYZS800 and NiOYSZ1000. The nominal weight ratio of NiO/YSZ was 56/44. After impregnation, the composites were dried at 280 °C for 4 h and calcinated at 800 °C for 8 h.

Slurries of NiO/YSZ powders were prepared using reagent grade organic additives. Ethylene glycol was used as a solvent and plasticizer, Triton X-100 [polyoxyethylene (10) isooctylphenyl ether] the tensioactive, menhaden fish oil (MFO) the dispersant, and poly(methyl methacrylate) (PMMA) was used as binder. Four samples of each compound, NiOYZS800 and NiOYSZ1000, were prepared using the identical composition and were submitted to milling times of 5, 10, 20 and 40 h in a ball mill that contained zirconia balls.

The slurries were deposited by spray coating [24] on commercial YSZ pellets (TZ8Y, Tosoh Corp., Japan) [34] using a Lince model MP5 spray. The sinterization of films was performed in air at 1150 °C for 6 h. Table 1 gives the symbols used to denote the films obtained from slurries prepared with different milling times.

The thickness of the layer deposited was about 10 μm for all films. Fig. 1 shows the interface between anode and YSZ substrate for sample L2.

2.2. Powder and slurry characterizations

The crystallographic characterizations of YSZ and their NiO/YSZ compounds were performed by X-ray diffraction (XRD) in a Rigaku diffractometer (GeigerflexModel, semi-automatic) equipped with Cu K_α radiation. The YSZ and NiO crystallite size were determined by means of the Scherrer equation [35], $D = 0.9\lambda/\beta\cos\theta$, where D is the crystallite size, λ is the wavelength of the radiation (1.5418 Å for Cu K_α radiation), β is corrected peak width at half-maximum intensity, and θ is the peak position.

The specific surface area, A, of YSZ powders calcinated at 800 and 1000 °C was determined by the multipoint Brunauer–Emmett–Teller (BET) nitrogen absorption method using a Quantachrome NOVA 1200 apparatus.

YSZ average particle sizes (d) were estimated by means of the equation: $d = 6/\rho A$ [36], where 6 is a constant, A is the specific area calculated from BET data, and ρ is the theoretical density of the material calculated by the equation $\rho = ZM/N_A V$ [36], with Z representing the number of formula units in the unit cell, M representing the formula weight, N_A representing the Avogadro's number and V representing the unit cell volume (V was calculated using the lattice parameters determined from XRD data).

The rheological behavior of different slurries was determined at 25 °C with a Haake rheometer model using triplicate samples of 1 mL suspensions. Initially, samples were sheared with shear rate of 5 s^{-1} for 10 s. Viscosity versus shear rates upward and downward curves were then obtained in the shear range of 5–200 s^{-1} for 600 s. Microstructural analyses of anode films were performed by Scanning Electron Microscopy (SEM)

Table 1
Symbols used to characterize the films as a function of milling time.

Starting powder	Milling time (h)	Films
NiO/YSZ800	5	F1
	10	F2
	20	F3
	40	F4
NiO/YSZ1000	5	L1
	10	L2
	20	L3
	40	L4

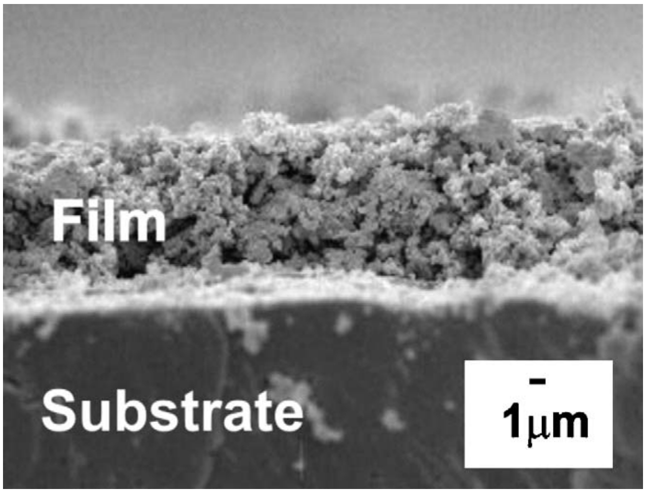

Fig. 1. SEM of the L2 anode film deposited on a YSZ substrate.

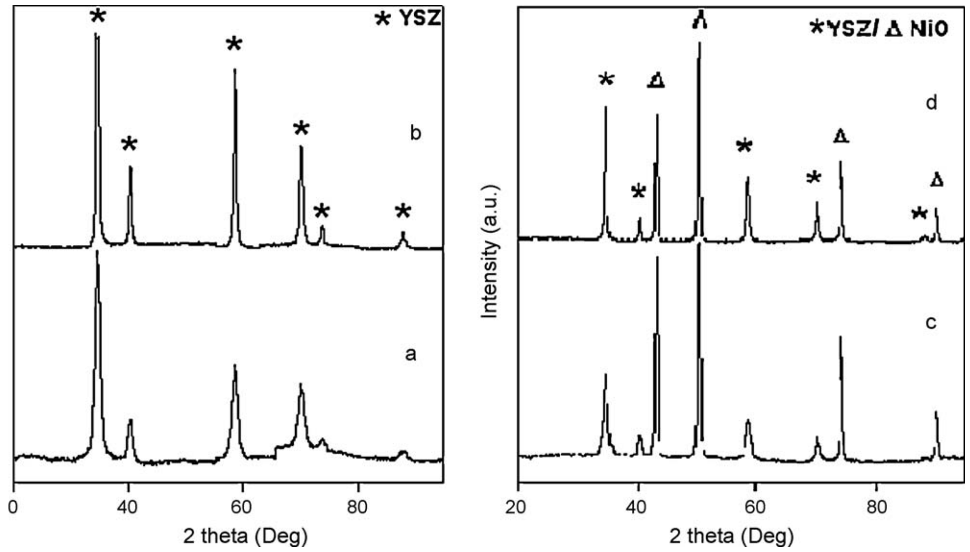

Fig. 2. XRD patterns of the powders (a) YSZ800, (b) YSZ1000, (c) NiO/YSZ800, and (d) NiO/YSZ1000.

using an electron microprobe analyzer apparatus (JEOL JSM-840A). For electron microscopy purposes, samples were coated with Au before the analyses.

3. Result and discussion

3.1. XRD analysis

Fig. 2 shows the XRD patterns obtained for samples YSZ800, YSZ1000 and their NiO composites NiO/YSZ800 and NiO/YSZ1000. The broadening of XRD lines and the higher background indicates the presence of amorphous phases, probably due to residual organic materials and/or size particles in the nanometer scale in the YSZ800 (Fig. 2(a)). After thermal treatment of YSZ powder at 1000 °C, the XRD patterns exhibited fine and well-defined lines, as shown in Fig. 2(b).

YSZ and NiO crystallite sizes for YSZ and YSZ/NiO samples estimated from XRD patterns are given in Table 2. The influence of calcination temperature on the crystallite size is clearly observed. YSZ powders treated at 1000 °C have YSZ crystallite sizes at least two times larger than those treated at 800 °C. Thermal treatment at 800 °C has not appreciable effect on YSZ crystallite sizes of both NiO/YSZ800 and NiO/YSZ1000 powders. In contrast, comparatively to NiO/YSZ800, the NiO crystallites of NiO/YSZ1000 increased about 70% when YSZ800 or YSZ1000 were used. The higher sinterability of NiO crystallites even at 800 °C is probably the cause for this effect. Moreover, YSZ crystallite sizes have a significant influence on the sinterability of the NiO particles since NiO crystallites were larger for samples with the larger YSZ particles. These results indicate that YSZ acts as a solid structure which inhibits and controls the crowing of NiO particles avoiding the NiO coalescence. The final network with YSZ and NiO arranged such as which material is in contact with other and also with itself is an ideal structure in which the percolation is maximized permitting electrical and ionic conductivity in electrode for the Ni and YSZ phases after reduction, respectively [37,38].

Table 2
YSZ and NiO crystallite sizes on YSZ and NiO/YSZ samples.

Samples	Crystallite sizes, D (nm)	
	YSZ	NiO
YSZ800	14	–
YSZ1000	34	–
NiO/YSZ800	16	56
NiO/YSZ1000	35	72

3.2. BET analysis

Table 3 gives the specific surface area, A, the total volume of pores, V, the average pore diameter, d_p, and the average particle size, d, estimated from BET analyses. As expected, the specific surface area and the total volume of pores are very influenced by calcination temperature. A significant decrease was observed in these values when the calcination temperature increased from 800 to 1000 °C. The results also show that the average pore diameters (d_p) for YSZ1000 and YSZ800 are smaller than the crystallite size of NiO particles, indicating that NiO could not be trapped into YSZ pores [19].

The average particle size of YSZ800 was estimated by BET analyses was about three times smaller than that for YSZ1000. The ratio, d/D, between particle size values from BET (d) and crystallite sizes (D) estimated from Scherrer formula, was 1.3 and 1.5 for YSZ800 and YSZ1000, respectively. These results show

Table 3
Specific surface area, A, average pore diameter, d_p, total volume of pores, V, and the average particle size, d, values for YSZ 800 and YSZ1000 powders.

Powders	A ($m^2 g^{-1}$)	d_p (nm)	V ($10^{-3} cm^3 g^{-1}$)	d (nm)
YSZ800	57	10	142	17
YSZ1000	19	6	26	52

Error: ±5%.

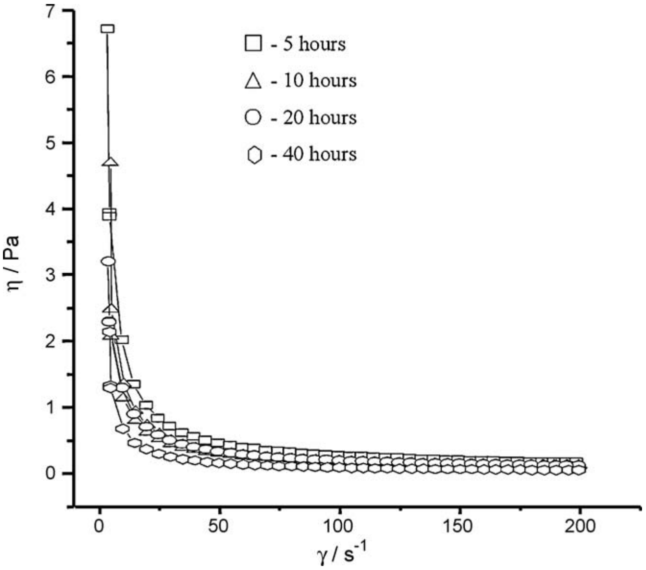

Fig. 3. Viscosity (η) as a function of shear rate (γ) curves for slurries produced from NiO/YSZ800.

that the YSZ powders presented some crystallite agglomeration after calcination. The 1.3 and 1.5 results show that YSZ1000 has highest crystallite quantities in its particle than YSZ800. It occurs because in 1000 °C occur more particle growing.

3.3. Rheology

Figs. 3 and 4 show typical curves of viscosity (η) as a function of shear rate (γ) for slurries produced from NiO/YSZ800 and NiO/YSZ1000 milled for 5,10, 20 and 40 h. All slurries presented pseudoplastic behavior in which the viscosity decreases with shear rate. Many complex suspensions in which inorganic and polymers materials are put together present this behavior [39–41]. The increasing the shear rate induces a more oriented particle alignment causing the decreasing of viscosity. This effect is more clearly observed for slurries prepared from YSZ800 powders than to that YSZ1000 ones. This pseudoplastic behavior is desirable to spray coating technique. The decrease in viscosity with shear rate is easier to conduct the slurry through the aerograph forming anode film in the substrate. The stress using for deposition of the film is sufficient to reach the pseudoplastic behavior of the slurry. The Newtonian region is reaching for NiO/YSZ800 slurry in shear rate in the range from 40 to 50 s^{-1} in milling time from 40 to 5 h respectively. In NiO/YSZ1000, the Newtonian region is reaching from 25 to 76 s^{-1} in milling time from 40 to 5 h respectively. It cannot observe a big difference between slurries milled in 10 and 20 h neither NiO/YSZ800 nor NiO/YSZ1000 slurries. In this shear rate region, the viscosities are from 0.46 to 0.20 Pa s for NiO/YSZ800 slurries and from 0.37 to 0.12 Pa s from NiO/YSZ1000 slurries. The least viscosity value indicates the more stability of the slurry. A good stability of the slurry is important to reach a desirable microstructure on the anode films. Then the rheological measurements are important to give information about the suspensions stability. The morphology of anode films defines the anode electrical response and so it is very important to optimize it. The results show that NiO/YSZ1000 slurries had smaller viscosity being more stable. The viscosity differences among slurries milled in 10, 20 and 40 h suggest that the slurry NiO/YSZ1000 with 20 h of milling was the optimized slurry. The higher milling time (40 h) did not cause alterations in the slurry viscosity and the slurry prepared using 10 h of milling time has a higher and unfavorable thixotropy.

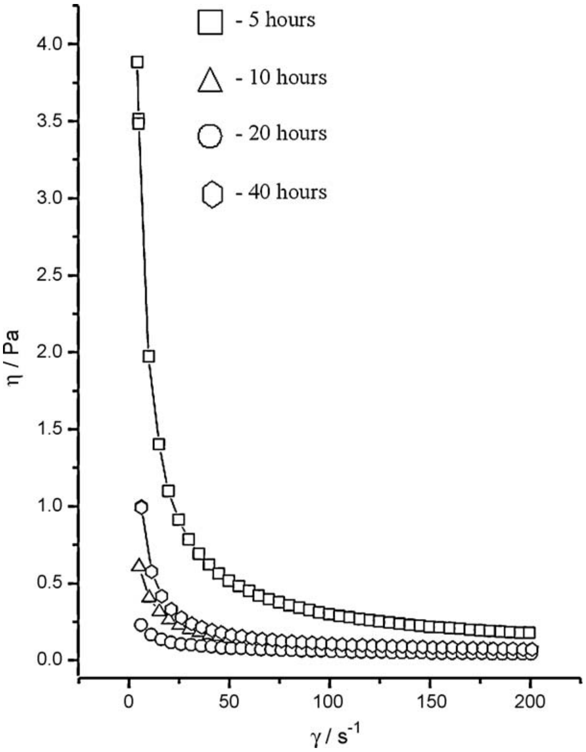

Fig. 4. Viscosity (η) as a function of shear rate (γ) curves for slurries produced from NiO/YSZ1000.

Samples presented also a time-dependent behavior. The longer the slurries undergo shear stress, the lower their viscosity which characterize the thixotropic fluids. NiO/YSZ1000 samples milling for 5 and 10 h present highest thixotropic area than that corresponding to NiO/YSZ800. The difference reaches 84% but for milling time of 20 h this situation inverses. These results show that the time required to the reorganization of system to initial condition is larger for samples in which the particle size is bigger for milling time down to 20 h but after this time period, the NiO/YSZ1000 samples present smaller thixotropy. The thixotropy occurs because the polymer chain organizes in the bulk of slurries forming tridimensional structures. During the shearing this structures are destroyed, carrying a viscosity decrease. After sometime the polymer chain organizes again. The thixotropy is desirable in spray coating technique to avoid that slurry drain in the substrate.

Fig. 5 shows the micrograph of the NiO/YSZ1000 sample milling for 20 h (L3) after deposition in YSZ substrate by spray coating and thermal treatment.

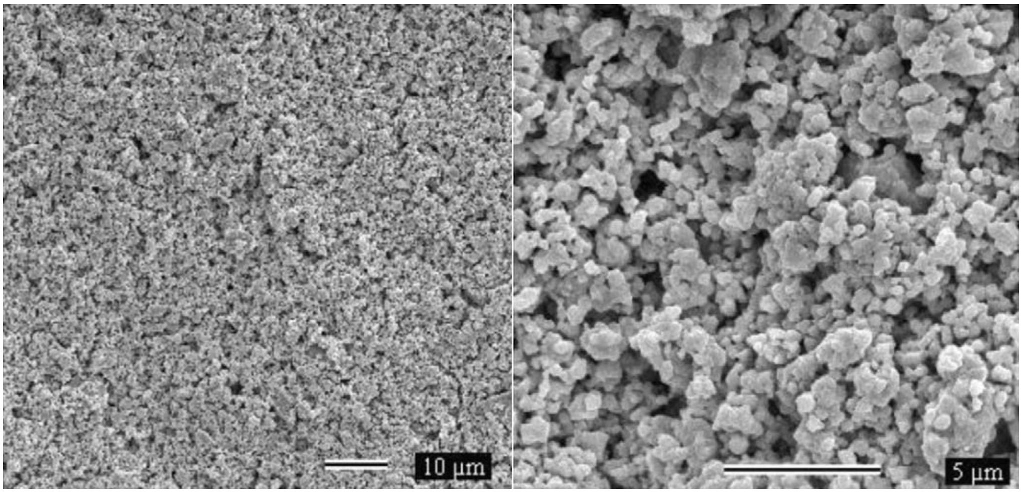

Fig. 5. Micrograph of sample L3.

4. Conclusion

This work showed that the calcination temperature and consequently the powder particle size are essential parameters to be focused when anode SOFC films are prepared by spray coating process. Suspensions with lower viscosity and lower degree of thixotropy were obtained with samples prepared using YSZ powders calcinated at 1000 °C. It was possible to define the better milling time, 20 h in the present study, for the system studied. The slurries showed pseudoplastic behavior, which is desirable in spray coating technique. The rheological results gave important information about suspensions' stability once the morphology and microstructure of anode films influence significantly their electrical response. Although for each system the set of experimental conditions must be considered, the present work give an insight into how to utilize the rheological behavior of slurries in order to predict the best materials to be used in spray coating process for SOFC anodes.

Acknowledgements

This work was supported by Fundação de Amparo a Pesquisa de Minas Gerais (FAPEMIG) and the Companhia Energética de Minas Gerais (CEMIG).

References

[1] A.B. Stambouli, E. Traversa, Renew. Sustain. Energ. Rev. 6 (2002) 433.
[2] D. Simwonis, H. Thülen, F.J. Dias, A. Naoumidis, D. Stöver, J. Mater. Process. Technol. 92/93 (1999) 107.
[3] N.Q.J. Minh, Am. Ceram. Soc. 76 (1993) 563.
[4] E. Ivers-Tiffée, A. Weber, D.J. Herbstritt, Eur. Ceram. Soc. 21 (2001) 1805.
[5] S.H. Chan, H.K. Ho, Y.J. Tian, Power Sources 109 (2002) 111.
[6] W. Winkler, H.J. Lorenz, Power Sources 105 (2002) 222.
[7] R.N. Basu, G. Blass, H.P. Buchkremer, et al. Eur. Ceram. Soc. 25 (2005) 463.
[8] Y.B. Matus, L.C. De Jonghe, C.P. Jacobson, et al. Solid State Ionics 176 (2005) 443.
[9] H.Y. Jung, W.S. Kim, S.H. Choi, et al. J. Power Sources 155 (2006) 145.
[10] H. Abe, K. Murata, T. Fukui, et al. Fuel Cell Bull. 2006 (2006) 12.
[11] X. Zhang, S. Ohara, R. Maric, et al. Power Sources 83 (1999) 170.
[12] S.K. Pratihar, A. Das Sharma, R.N. Basu, et al. Power Sources 129 (2004) 138.
[13] F.H. Wang, R.S. Guo, Q.T. Wei, et al. Mater. Lett. 58 (2004) 3079.
[14] R.J. Gorte, J.M. Vohs, J. Catal. 216 (1–2) (2003) 477–486.
[15] S.T. Aruna, M. Muthuraman, K.C. Patil, Solid State Ionics 111 (1998) 45.
[16] C.H. Lee, C.H. Lee, H.Y. Lee, et al. Solid State Ionics 98 (1997) 39.
[17] W.Z. Zhu, S.C. Deevi, Mater. Sci. Eng. 362 (2003) 228.
[18] S.P. Jiang, Mater. Sci. Eng. 418 (2006) 199.
[19] S. Suda, M. Itagaki, E. Node, et al. Eur. Ceram. Soc. 26 (2006) 593.
[20] D. Simwonis, F. Tietz, D. Stöver, Solid State Ionics 132 (2000) 241.
[21] H. Koide, Y. Someya, T. Yoshida, T. Maruyama, Solid State Ionics 132 (2000) 253.
[22] K.V. Jensen, R. Wallenberg, I. Chorkendorff, et al. Solid State Ionics 160 (2003) 27.
[23] K.C. Wincewicz, J.S.J. Cooper, Power Sources 140 (2005) 280.
[24] Y.J. Leng, S.H. Chan, K.A. Khor, et al. J. Power Sources 117 (2003) 26.
[25] A. Mukherjee, B. Maiti, A. Das Sharma, et al. Ceram. Int. 27 (2001) 731.
[26] F. Snijkers, A. de Wilde, S. Mullens, et al. Eur. Ceram. Soc. 24 (2004) 1107.
[27] S. Zürcher, T. Graule, J. Eur. Ceram. Soc. 25 (2005) 863–873.
[28] L.A. Salam, R.D. Matthews, H. Robertson, Mater. Chem. Phys. 62 (2000) 263–272.
[29] Z. Xu, G. Rajaram, D. Pai, J. Sankar, Ceram. Eng. Sci. Proc. (2005).
[30] Y. Liu, L.E. Lao, Solid State Ionics 177 (2006) 159.
[31] A. Ghosh, A.K. Suri, M. Pandey, et al. Mater. Lett. 60 (2006) 1170.
[32] H. Mori, C.J. Wen, J. Otomo, et al. Appl. Catal. 245 (2003) 79.
[33] C.M. Finnerty, N.J. Coe, R.H. Cunningham, et al. Catal. Today 46 (1998) 137.
[34] M. C. Steil, Ph.D. thesis, Ecole Nationale Supérieure des Mines de Saint-Étienne and Ecole Centrale de Lyon, Saint-Étienne/Lyon, France, 1996.
[35] Ja. Dhahri, S. Zemni, K. Cherif, et al. Alloy. Compd. 394 (2005) 51.
[36] G.E. Lascalea, D.G. Lamas, E. Djurado, et al. Mater. Res. Bull. 40 (2005) 2029.
[37] J.-H. Lee, H. Moon, H.-W. Lee, J. Kim, K.-H. Yoon, Solid State Ionics 148 (1–2) (2002) 15–26.
[38] G. Rajaram, S. Desai, Z. Xu, M. Devdas, J. Sankar, Int. J. Manuf. Res. 3 (3) (2008) 350–359.
[39] Z.Z. Yi, Z.P. Xie, Y. Huang, J.T. Ma, Y.B. Cheng, Ceram. Int. 28 (2002) 369–376.
[40] I.M.G. Santos, A.G. Souza, F.R. Sensato, E.R. Leite, E. Longo, J.A. Varela, J. Eur. Ceram. Soc. 22 (2002) 1297–1306.
[41] S. Rossi, P.F. Luckham, Th.F. Tadros, Colloid Surf. A: Physicochem. Eng. Aspects 201 (2002) 85–100.